Distribution of Colloidal Particles in a Spherical Cavity

Jyh-Ping Hsu* and Ji-Ming Jiang

Department of Chemical Engineering, National Taiwan University, Taipei, Taiwan 10617

Shiojenn Tseng

Department of Mathematics, Tamkang University, Tamsui, Taipei, Taiwan 25137

Bo-Tau Liu†

Daxon Technology Inc., Taoyuan, Taiwan 33341

Received: March 6, 2005; In Final Form: July 31, 2005

The spatial distribution of colloidal particles in a confined space is frequently a key issue to many phenomena of practical significance. This problem is investigated by considering the distribution of colloidal particles in a spherical cavity under the conditions of relatively large cavities, low cavity and colloidal particles potentials, and low monovalent electrolyte and colloidal concentrations. The analytical expression for the particle−cavity pair interaction energy is derived under various surface conditions. The results obtained are used to evaluate the direct correlation functions in the hypernetted chain approximation employed for the resolution of an Ornstein−Zernike equation. For a fixed particle number concentration at the center of a cavity, we make the following conclusions: (i) the spatial distribution of particles increases in an oscillatory manner with the distance away from the cavity surface, (ii) increasing the particle−cavity pair interaction energy has the effect of reducing the free space of particles inside a cavity, and (iii) the greater the pair interaction energy between two particles, the higher the average concentration of particles.

1. Introduction

In the past few decades, the physical properties of fluids confined in a narrow space such as slits or pores have drawn the attention of researchers in various fields. This arises from their association with practical applications such as the exhausted gas treatment by active carbon fibers, the desalination of water through ion-exchange resins, as well as their relevance to phenomena such as selective adsorption from mixtures, the long-range depletion force between two relatively large entities, to name a few.[1−6] In these cases, the entity−entity and entity−boundary interactions generally yield an inhomogeneous spatial distribution of fine entities. Van Winkle and Murray,[7] for example, observed experimentally the distribution of latex particles near a smooth repulsive glass wall. It was found that the concentration of particles increases oscillatory with the distance away from the wall. The developments in density functional theory[8] and integral equation based formalisms[9] facilitate theoretical study on the concentration profile of charged entities near the dispersion medium-wall interfaces of a confined space. In the former, the grand potential of a system is expressed as a function of particle density distribution, and the minimization of this potential leads to the equilibrium density distribution of the system. Choudhury and Ghosh,[10] for instance, investigated the nature of a colloidal dispersion in a charged cylindrical pore. Adopting a perturbative density functional approach, they obtained the density distribution of particles, and showed that the contribution of salts can be taken into account by including higher order correlation terms. In an integral equation approach, one solves the Ornstein−Zernike equation along with a suitable closure, such as hypernetted chain, Percus−Yevick, or mean spherical approximation, for both wall-particle and particle−particle correlations. Chavez-Paez et al.,[11] for example, used this approach to study the behavior of a colloidal dispersion in a charged cylindrical pore. Their results are consistent, in general, with those obtained by computer simulations, although the peak heights of the concentration profile are a bit underestimated. Hsu et al.[12] examined the distributions of colloidal particles in various two-dimensional energy fields through an integral equation approach. It was found that the qualitative behavior predicted agrees well with that observed by Van Winkle and Murray.[7] The integral equation approach was also adopted often to determine the ion distribution in an electrical double layer. Lozada-Cassou,[13] for example, used the hypernetted chain closure associated with a mean spherical approximation to calculate the ion distribution near a cylindrical electrode. It was shown that, if the linear size of an ion is infinitely small, and the radius of the electrode approaches infinity, the result reduces to that predicted by the classic Gouy−Chapman theory. Zaini et al.[14] used the same approach to evaluate the distribution of ions in a cylindrical pore. A bridge function is proposed to correct the deviation arising from the negligence of some of the integral graphs in the cluster diagram. Yeomans et al.[15] investigated the distribution of ions within and surrounding a charged cylindrical pore by adopting a hypernetted chain/mean spherical approximation closure. They concluded that the result obtained differs both quantitatively and qualitatively from that based on the classic Poisson−Boltzmann theory, especially for small pores. The hypernetted chain approach was

* To whom correspondence should be addressed. Fax: 886-2-23623040. E-mail: jphsu@ntu.edu.tw.

† Telephone: 886-3-374-8800. Fax: 886-3-374-8888. E-mail: btliu@ntu.edu.tw.

10.1021/jp051151x CCC: $30.25
Published on Web 08/31/2005

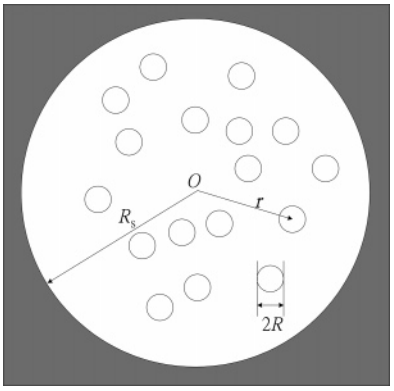

Figure 1. Schematic representation of the system under consideration, where open circles represent colloidal particles and shaded area denotes spherical cavity, *r* is the vector from the center of the cavity to that of a colloidal particle.

also adopted to evaluate the electrical interaction between two charged surfaces.[16−19]

In this study, the distribution of colloidal particles in a spherical cavity is discussed under the conditions of relatively large cavities, low cavity and colloidal particles potentials, and low monovalent electrolyte and colloidal concentrations. Analytical expression for the particle−cavity pair interaction energy is derived under various surface conditions, and the set of hypernetted chain equations describing the variations of the correlation functions for particle−particle and particle−cavity interactions are solved numerically based on a discrete Fourier transform coupled with a Newton−Raphson iteration scheme.

Au: Please note the following. Do not stack exponents (as in the equations below). Also, in our style, equations must be consecutively numbered/lettered. Using eq 1, 1a, 1b, etc. is not allowed. Use eq 1a, 1b, 1c, etc.

2. Analysis

The problem under consideration is illustrated in Figure 1 where monodispersed colloidal particles (*c*) with a scaled radius R are dispersed in a rigid, spherical cavity (*s*) with a scaled radius R_s filled with an electrolyte solution. The spatial distribution of colloidal particles is characterized by the density distribution function, $\rho(r)$, as[20]

$$\rho(r) = \rho_0 g_{sc}(r) \tag{1a}$$

where ρ_0 and $g_{sc}(r)$ are respectively the number concentration of colloidal particles at the center of a cavity ($r = 0$) and the radial distribution function. Here, r is the vector from the center of the cavity, scaled by ${\rho_0}^{-1/3}$, that is

$$\mathbf{r} = r{\rho_0}^{1/3} \tag{1b}$$

$\mathbf{r}$ being the scaled vector connecting a colloidal particle and the cavity. Since only one cavity is present in the present system, $g_{sc}(\mathbf{r})$ can be determined by the Ornstein−Zernike equations[20]

$$h_{cc}(\mathbf{r}) = c_{cc}(\mathbf{r}) + \int_V h_{cc}(\mathbf{r}')c_{cc}(\mathbf{r} - \mathbf{r}')\,\mathrm{d}\mathbf{r}' \tag{2a}$$

$$h_{sc}(\mathbf{r}) = c_{sc}(\mathbf{r}) + \int_V h_{sc}(\mathbf{r}')c_{cc}(\mathbf{r} - \mathbf{r}')\,\mathrm{d}\mathbf{r}' \tag{2b}$$

with

$$h_{ij}(\mathbf{r}) = g_{ij}(\mathbf{r}) - 1, \quad i,j = s,c \tag{2c}$$

The integrals in eq 2, parts a and b, are performed over the space inside the cavity, and $c_{ij}(\mathbf{r})$ and $h_{ij}(\mathbf{r})$ are respectively the direct and indirect correlation functions between entities *i* and *j*. Employing the hypernetted-chain approximation (HNC),[20] we have

$$c_{ij}^{HNC}(\mathbf{r}) = h_{ij}(\mathbf{r}) - \ln[1 + h_{ij}(\mathbf{r})] - u_{ij}(\mathbf{r})/k_BT \tag{3}$$

where $u_{ij}(\mathbf{r})$ is the pair interaction energy between entities *i* and *j*, and k_B and T are respectively the Boltzmann constant and absolute temperature. Equations 2a, 2b, and 3 lead to two independent problems. First, given ρ_0 and $u_{cc}(\mathbf{r})$, these equations can be solved for $h_{cc}(\mathbf{r})$ and $c_{cc}^{HNC}(\mathbf{r})$. It can be shown that

$$h_{cc}(\mathbf{r}) = c_{cc}^{HNC}(\mathbf{r}) + h_{cc}(\mathbf{r}) * c_{cc}^{HNC}(\mathbf{r}) \tag{4}$$

where $*$ denotes the convolution operator. Second, given $c_{cc}^{HNC}(\mathbf{r})$ and $u_{sc}(\mathbf{r})$, eqs 2a, 2b, and 3 can be solved for $h_{sc}(\mathbf{r})$ and $c_{sc}^{HNC}(\mathbf{r})$, and we have

$$h_{sc}(\mathbf{r}) = c_{sc}^{HNC}(\mathbf{r}) + h_{sc}(\mathbf{r}) * c_{cc}^{HNC}(\mathbf{r}) \tag{5}$$

For spherical particles, both $h_{cc}(\mathbf{r})$ and $c_{cc}^{HNC}(\mathbf{r})$ are functions of the distance between two particles only, and the vector $\mathbf{r}$ can be replaced by its magnitude r.

Following the treatment of Broyles et al.,[21] eq 4 is solved by first extending the domain of $h_{cc}(r)$ and $c_{cc}^{HNC}(r)$ from $[0,\infty)$ to $(-\infty,\infty)$ through defining

$$h_{cc}(r) = h_{cc}(-r), \quad r \in (-\infty,0] \tag{6a}$$

$$c_{cc}^{HNC}(r) = c_{cc}^{HNC}(-r), \quad r \in (-\infty,0] \tag{6b}$$

Also, we define

$$H_{cc}(r) = r[h_{cc}(r) - c_{cc}^{HNC}(r)] \tag{7a}$$

$$I_{cc}(r) = -rc_{cc}^{HNC}(r) = H_{cc}(r) - rh_{cc}(r) \tag{7b}$$

$$J_{cc}(r) = -\int_{-\infty}^{r} I_{cc}(s)\,\mathrm{d}s \tag{7c}$$

On the basis of these expressions, eq 4 can be rewritten as

$$H_{cc}(r) = 2\pi[\int_{-\infty}^{\infty} I_{cc}(r')J_{cc}(r - r')\,\mathrm{d}r' - \int_{-\infty}^{\infty} H_{cc}(r')J_{cc}(r - r')\,\mathrm{d}r'] \tag{8}$$

Equations 8 and 3 can be transformed to discrete forms as

$$H_{cc,n} = 2\pi\delta[\sum_{n'=-N}^{N} I_{cc,n'}J_{cc,(n-n')} - \sum_{n'=-N}^{N} H_{cc,n'}J_{cc,(n-n')}] \tag{9a}$$

$$h_{cc,n} = -1 + \exp\left[\frac{H_{cc,n}}{n\delta} - \frac{u_{cc,n}}{k_BT}\right] \tag{9b}$$

In these expressions, δ is a discretizing interval, and N is an integer sufficiently large ($N \le R_s/\delta$) such that $H_{cc,n} \approx 0$ for $|n| > N$. The following iterative procedure can be used to solve parts a and b of eq 9 simultaneously. Step 1: guess an initial $H_{cc,n}$ and substitute it into eq 9b to evaluate $h_{cc,n}$. Step 2: substitute $h_{cc,n}$ obtained into eq 7b, and insert the resultant expression into eq 7c to obtain $I_{cc,n}$ and $J_{cc,n}$. Step 3: substitute these $I_{cc,n}$ and $J_{cc,n}$ values into eq 9a, and take the discrete Fourier transform on the resultant expression to obtain

$$\hat{H}_{cc,k} = \frac{2\pi \hat{I}_{cc,k} \hat{J}_{cc,k}}{1 + 2\pi \hat{J}_{cc,k}}, \quad -\infty < k < \infty \tag{10}$$

where $\hat{F}_k$ is the Fourier transform coefficient of F_n. Step 4: take the inverse transform of $\hat{H}_{cc,k}$ to obtain $H_{cc,n}$ and substitute the resultant expression into eq 9b to obtain a modified $h_{cc,n}$. Steps 1−4 are repeated until a self-consistent $H_{cc,n}$ is obtained. $F(r)$ is then recovered from F_n through using a linear interpolation method. We find that $H_{cc}(r)$, $I_{cc}(r)$, $J_{cc}(r)$ are negligible for $|r| \geq 6R$.

Because of spherical geometry, both $h_{sc}(r)$ and $c_{sc}^{HNC}(r)$ in eq 5 are also functions of r. Therefore, $h_{sc}(r)$ and $c_{sc}^{HNC}(r)$ can be expanded as

$$h_{sc}(r) = \sum_{n=1} h_{sc,n} L_n(r, r_n) \tag{11}$$

$$c_{sc}^{HNC}(r) = \sum_{n=1} c_{sc,n}^{HNC} L_n(r, r_n) \tag{12}$$

where n is the nth node of r, $h_{sc,n}$ is the value of $h_{sc}(r_n)$, and L_n denotes the Lagrange interpolation function. As indicated by Zaini et al.,[14] the resolution of eq 5 can be accomplished by letting the residuals vanish at all the nodes, and we have

$$h_{sc,n} = c_{sc,n}^{HNC} + \sum_{j=1} \Delta_r \cdot h_{sc,j} \int_0^{R_s} c_{cc}^{HNC}(\sqrt{(r_n - r_j)^2 + \tau^2}) d\tau \tag{13a}$$

$$c_{sc,n}^{HNC} = h_{sc,n} - \ln(1 + h_{sc,n}) - u_{sc,n}/k_B T \tag{13b}$$

where Δ_r is the discretizing interval of r. Note that the problem defined by these two equations is nonlinear. Equation 13a can be rewritten as

$$[Q][h_{sc}] = [h_{sc}] - [c_{sc}^{HNC}] \tag{14a}$$

where

$$[Q]_{ij} = \Delta_r \cdot \int_0^{R_s} c_{cc}^{HNC}(\sqrt{(r_i - r_j)^2 + \tau^2}) d\tau \tag{14b}$$

$$[h_{sc}]_i = h_{sc,i} \tag{14c}$$

$$[c_{sc}^{HNC}]_i = c_{sc,i}^{HNC} \tag{14d}$$

Substituting eq 14a into eq 13b leads to

$$[h_{sc}] = \exp([Q][h_{sc}] - [u_{sc}]) - [111\cdots111]^T \tag{15a}$$

where T denotes matrix transpose, and

$$[u_{sc}]_i = u_{sc,i} \tag{15b}$$

$$\exp([x])_i = \exp([x]_i) \tag{15c}$$

Equation 15a is solved by the Newton−Raphson method through using the iterative expression

$$[h_{sc}^{\gamma}]_{(k+1)} = [h_{sc}^{\gamma}]_{(k)} - [S][-1 + \exp(\gamma[Q][h_{sc}^{\gamma}]_{(k)} - [u_{sc}]) - [h_{sc}^{\gamma}]_{(k)}] \tag{16}$$

where $[h_{sc}^{\gamma}]_{(k)}$ denotes the kth iterative solution with parameter γ, $0 < \gamma \leq 1$, and

$$[S] = ([Q] \otimes [\exp(\gamma[Q][h_{sc}]_{(k)} - [u_{sc}]) \times [111\cdots11]] - [I])^{-1} \tag{17a}$$

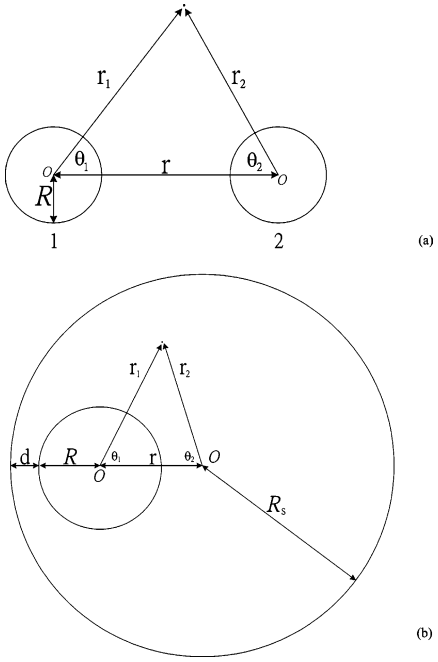

Figure 2. Coordinates used for the description of particle−particle interaction (a) and particle−cavity interaction (b).

The operator $\otimes$ has the property

$$[a] \otimes [b] = [c], \; c_{ij} = a_{ij} b_{ij} \tag{17b}$$

The parameter γ is designed to improve the performance of the iteration, which comprises the following steps. Step 1: assign a small value, e.g., 0.1, to γ, and make the initial guess

$$[h_{sc}^{\gamma}] = \exp(-[u_{sc}]) - [111\cdots111]^T \tag{18}$$

Step 2: substitute this expression into eq 16, and evaluate $[h_{sc}^{\gamma}]_{(1)}$. Repeat this step until a convergent expression, $[h_{sc}^{\gamma}]_{(\infty)}$, is obtained. Step 3: increase the value of γ, use $[h_{sc}^{\gamma}]_{(\infty)}$ as the initial guess, and return to step 1. This is repeated until $[h_{sc}^{1.0}]_{(\infty)}$ is obtained.

2.1. Pair Interaction Energies, u_{cc} and u_{sc}. To evaluate the direct correlation functions, c_{cc}^{HNC} and c_{sc}^{HNC}, the pair interaction energies, u_{cc} and u_{sc}, in eqs 9b and 13b need to be known. Here, we consider two cases: (i) both particle surface and cavity surface are remained at constant potential; (ii) the surface of a particle remained at a constant potential and that of the cavity is of a charge-regulated nature. If we refer to Figure 2a, the pair interaction energy between two particles with a center-to-center distance r can be derived based on a charging procedure or a coupling constant integration as[22]

$$u_{cc}(r) = 4\pi R \epsilon \psi_1^2 \left[\frac{-\pi \alpha_0}{2\psi_1 \sinh(\kappa R)} + \kappa R + \kappa R \coth(\kappa R) \right] \tag{19}$$

where ϵ is the relative permittivity of the electrolyte solution, and ψ_1 is the scaled surface potential of a particle. Note that because α_0 varies with r, eq 19 is an implicit relation between u_{cc} and r. A procedure to evaluate α_0 is given in Appendix A.

By referring to Figure 2b, the pair interaction energy u_{sc} can be derived through a similar procedure as that employed in the derivation of u_{cc}. Applying collocation method, u_{sc} can be expressed as a sum of the surface integrals over each surface[23]

$$u_{sc}(d) = 2\pi R^2 \int_{-1}^{1} u_c(d, \mu_c) \, d\mu_c + 2\pi R_s^2 \int_{-1}^{1} u_s(d, \mu_s) \, d\mu_s \tag{20}$$

where $d = R_s - R - r$ is the distance of closest approach between the surface of a colloidal particle and the cavity, $u_c(d,\mu_c)$ and $u_s(d,\mu_s)$ are respectively the interaction energy per unit area at position $(\mu_c,\mu_s) = (\cos\theta_1,\cos\theta_2)$ on particle surface and cavity when they are at a distance d apart. Both $u_c(d,\mu_c)$ and $u_s(d,\mu_s)$ are functions of the charged conditions on surfaces. It can be shown that if both particle surface and cavity surface are remained at constant potential, employing $\psi = \psi_1$ at $r_1 = R$ and $\psi = \psi_2$ at $r_2 = R_s$, then

$$u_c(d,\mu_c) = \frac{2\pi\epsilon\psi_1}{\kappa}\left(\frac{k_BT}{e}\right)^2\left[(\kappa R)^2\frac{\exp(\kappa R)}{\sinh(\kappa R)}\psi_1 - \frac{\pi\alpha_0}{2i_0(\kappa R)}\right] \quad (21)$$

$$u_s(d,\mu_s) = \frac{2\pi\epsilon\psi_2}{\kappa}\left(\frac{k_BT}{e}\right)^2\left[(\kappa R_s)^2\frac{\exp(\kappa R_s)}{\sinh(\kappa R_s)}\psi_2 - \frac{\pi\beta_0}{2k_0(\kappa R_s)}\right] \quad (22)$$

The values of α_0 and β_0 can be determined by the procedure summarized in Appendix B. If the surface of cavity is of charge-regulated nature, then it can be shown that the $u_s(d,\mu_s)$ in eq 20 becomes

$$u_s(d,\mu_s) = 2\pi\epsilon R_s\psi_2\left(\frac{k_BT}{e}\right)^2\left(1 + \kappa R_s + \frac{R_sK}{\epsilon}\right) \times \left\{\frac{k_0(\kappa R_s)}{\left[\frac{R_sK}{\epsilon}k_0(\kappa R_s) - \kappa R_s k_0'(\kappa R_s)\right]} - \frac{i_0(\kappa R_s)}{\left[\frac{R_sK}{\epsilon}i_0(\kappa R_s) - \kappa R_s i_0'(\kappa R_s)\right]}\right\} \times \left\{\psi_2\left(-1 - \kappa R_s + \frac{R_sK}{\epsilon}\right) - \beta_0\left[\frac{R_sK}{\epsilon}i_0(\kappa R_s) - \kappa R_s i_0'(\kappa R_s)\right]\right\} \quad (23)$$

where β_0 can be calculated by the procedure summarized in Appendix B. Applying eq 20 with $r = R_s - R - d$, the pair interaction energy $u_{sc}(r)$ for the case when the particle is remained at constant potential and cavity surface is of charge-regulated nature can be evaluated. For a simpler presentation, the scaled u_{sc}, $U_{sc} = u_{sc}/\epsilon\kappa^{-1}(k_BT/e)^2$ is used in Figure 3.

3. Results and Discussion

The effects of the charged conditions on particle and cavity surfaces on the variation of the scaled pair interaction energy between a particle and the cavity U_{sc} as a function of the scaled particle−cavity distance d/R_s are presented in Figure 3. Figure 3a indicates that if both particle surface and cavity surface are remained at constant potential, U_{sc} decreases with the increase in d/R_s, for a fixed ψ_2 U_{sc} increases with the increase in ψ_1, and for a fixed cavity size, the larger the colloidal particle the greater the U_{sc} is. These behaviors are expected. Referring to eq B10, three types of charged conditions on particle surface are considered in Figure 3b: constant surface potential or ($K \to \infty$, $S \to \infty$), constant charge density with $(K,S) = (0,1)$, and charge-regulated with $(K,S) = (1,1)$. Figure 3b indicates that the magnitude of U_{sc} follows the order (constant charge) > (charge-regulated) > (constant potential), which is consistent with the result of Carnie et al.[22]

The spatial variations in the indirect correlation function h_{sc} as a function of r at various cavity sizes for the case when both particle and cavity surfaces are remained at a constant potential are presented in Figure 4. As can be seen in this figure, if r is sufficiently large, $h_{sc} = -1$, and if it is small, h_{sc} is of oscillatory nature and has a global maximum at a certain r. According to eqs 1 and 2c, this implies that the concentration of particles vanishes near cavity surface, it has a global maximum at a point $0 < r = r_{max} < R_s$, and it oscillates in the range $0 < r < r_{max}$. Figure 4 also reveals that the larger the cavity (or the smaller the particle), the smoother the distribution of h_{sc} near the center of the cavity, that is, the closer the present result to that for a

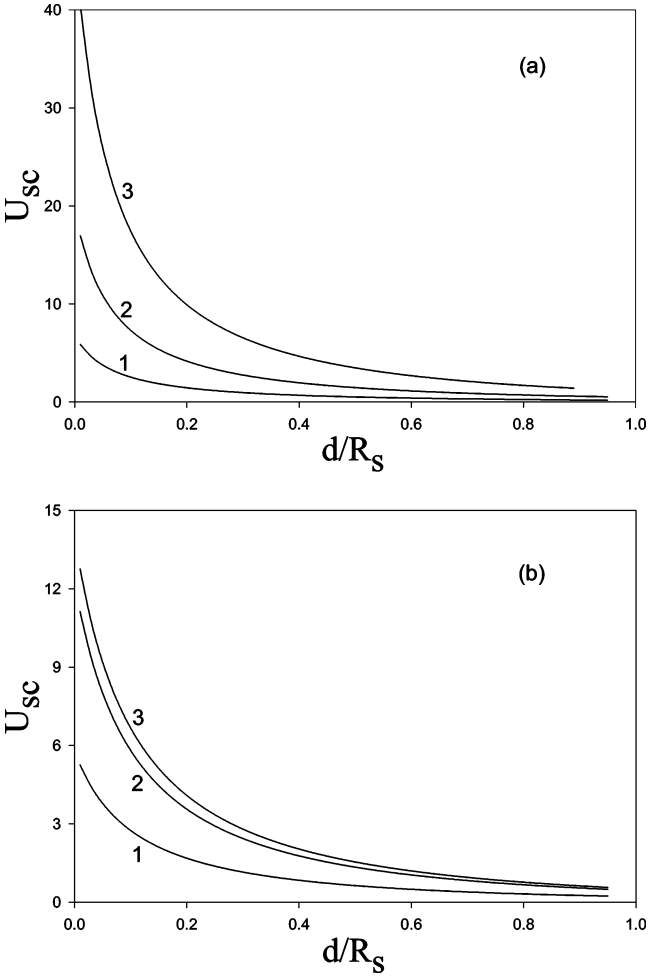

Figure 3. Effects of the charged conditions on particle and cavity surfaces on the variation of the scaled pair interaction energy between a particle and the cavity U_{sc} as a function of the scaled particle−cavity distance d/R_s where (a) both particle and cavity remained at constant surface potential. Curves 1 and 2, $R_s/R = 20$, 3, $R_s/R = 10$. Curves 1 and 3, $(\psi_1,\psi_2) = (1,1)$, 2, $(\psi_1,\psi_2) = (3,1)$. (b) $\psi_1 = 1$ and $R_s/R = 20$. Curve 1, ($K \to \infty$, $S \to \infty$), 2, $(K,S) = (1,1)$, 3, $(K,S) = (0,1)$. Key: liquid phase is a 0.01 M 1:1 electrolyte solution, $T = 300$K, $\epsilon = 7.08 \times 10^{-10}$ C/V/m, $\rho_0 = 6 \times 10^{23}$ no./m^3, and $R = 5$ nm.

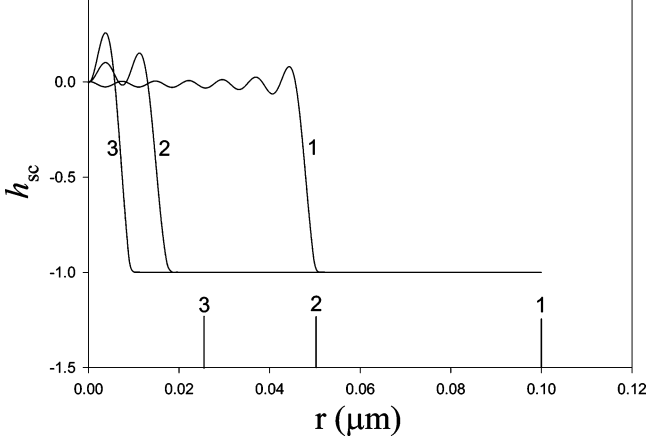

Figure 4. Variation of h_{sc} as a function of r at various cavity sizes for the case when $\psi_1 = \psi_2 = 1$. Curve 1, $R_s/R = 20$, 2, $R_s/R = 10$, 3, $R_s/R = 5$. Line segments 1, 2, and 3 denote respectively the positions of the cavity surfaces correspond to curves 1, 2, and 3. Key: same as in Figure 3.

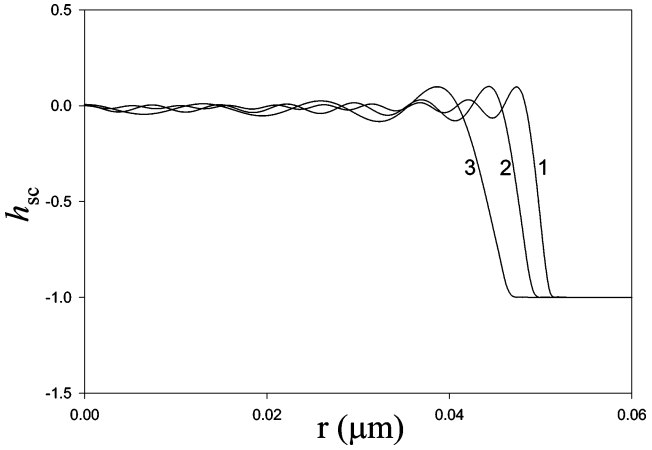

Figure 5. Variation of h_{sc} as a function of r at various interaction energy u_{sc}. Curve 1, $u_{sc}/u_{sc}^* = 1$, 2, $u_{sc}/u_{sc}^* = 2$, 3, $u_{sc}/u_{sc}^* = 4$, where u_{sc}^* is the value of u_{sc} calculated by eq 20 for the case when $R_s/R = 15$, $\psi_1 = 1$, and $(K,S) = (1,1)$. Key: same as in Figure 3.

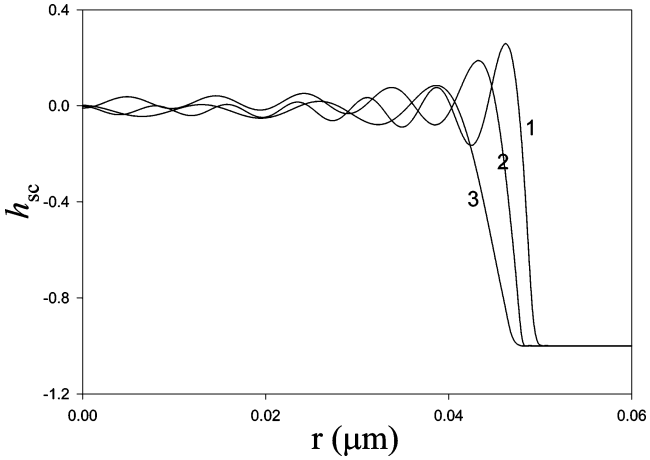

Figure 6. Variation of h_{sc} as a function of r at various interaction energy u_{cc}. Curve 1, $u_{cc}/u_{cc}^* = 2$, 2, $u_{cc}/u_{cc}^* = 1$, 3, $u_{cc}/u_{cc}^* = 0.5$, where u_{cc}^* is the value of u_{cc} calculated by eq 19 for the case when $R_s/R = 12$, $\psi_1 = 1$, and $(K,S) = (0,1)$. Key: same as in Figure 3.

planar slit.[12] This is expected because the larger the cavity, the less significant its curvature, and the closer the cavity to a planar surface. The average particle concentration inside the cavity can be evaluated by

$$\rho_{ave} = \frac{3}{4\pi R_s^3}\int_0^{R_s'} \rho_0(h_{sc} + 1)4\pi r^2 \, dr \qquad (24)$$

where R_s' is the value of R_s at which $h = -1$. The values of ρ_{ave} for curves 1, 2, and 3 in Figure 4 are, respectively, 4.84×10^{23}, 5.40×10^{23}, and 5.89×10^{23} no./m^3, that is, for a fixed number concentration of colloidal particles at the center of cavity ρ_0, the smaller the size of cavity the higher the ρ_{ave} is. The effect of the pair interaction energy u_{sc} on the distribution of colloidal particles in a cavity is illustrated in Figure 5. The values of ρ_{ave} for curves 1, 2, and 3 are, respectively, 5.65×10^{23}, 5.54×10^{23}, and 5.41×10^{23} no./m^3, that is, the smaller the interaction energy between particle and cavity u_{sc} the greater the average particle concentration inside a cavity. This is expected because for a fixed ρ_0, the smaller the u_{sc} the easier for particles to approach the surface of the cavity. Figure 5 also reveals that the greater the u_{sc} the smaller the r at which the global maximum of particle concentration occurs, but the global maximum is insensitive to the variation in u_{sc}. The variation of the indirect correlation function h_{sc} as a function of the center-to-center distance between a particle and the cavity r at various values of the interaction energy u_{cc} is presented in Figure 6. This figure indicates that the greater the u_{cc} the higher the average particle concentration inside a cavity. For example, the values of ρ_{ave} for curves 1, 2, and 3 are, respectively, 5.85×10^{23}, 5.74×10^{23}, and 5.61×10^{23} no./m^3. Also, the greater the u_{cc} the larger the global maximum of particle concentration and the larger the r at which the global maximum occurs.

Note that because the equation obtained by letting $i = c$ and $j = c$ in eq 3 is independent of that by letting $i = c$ and $j = s$, other closures can also be applied. For example, c_{cc}^{HNC} is replaced by that based on mean spherical approximation, and/or c_{sc}^{HNC} replaced by that based on Percus−Yevick approximation. It should be pointed out that the van der Waals interaction energy between two objects could also play a role. For simplicity, only the electrical interaction energy between two objects is considered in the present study. Also, it was pointed out that the charged conditions on the surface of a confined space could dramatically influence the pair interaction energy between two particles. The so-called proximity effect,[23,24] may result in a reduction, enhancement, or even elimination of the pair electrical interaction energy. In this case, the pair interaction energy between two particles needs to be modified appropriately.

4. Conclusion

In summary, the distribution of colloidal particles in a spherical cavity under the conditions of relatively large cavities, low cavity and colloidal particles potentials, and low monovalent electrolyte and colloidal concentrations is investigated by adopting a hypernetted-chain closure to evaluate the direct correlation functions for the particle−particle and particle−cavity interactions. Also, an analytical expression for the electrical energy for the latter is derived. If the surface of a cavity is remained at a constant potential, the magnitude of the particle−cavity interaction energy follows the order (particle surface is constant charge) > (particle surface is charge-regulated) > (particle surface is constant potential). For a fixed number concentration of particles at the center of a cavity, the spatial distribution of particle concentration is of oscillating nature, and has a global maximum. Also, the smaller the size of a cavity the higher the average particle concentration, the greater the particle−cavity interaction energy the lower the average particle concentration, and the greater the particle−particle interaction energy the higher the average particle concentration is.

Appendix A

Suppose that the electrical potential ψ outside two interacting particles can be described by the linearized Poisson−Boltzmann equation

$$\nabla^2\psi = \kappa^2\psi \qquad (A1)$$

where κ is the reciprocal Debye length. The solution to this equation can be expressed as[25,26]

$$\psi = \sum_{n=0}^{\infty}\alpha_n[k_n(\kappa r_1)P_n(\cos\theta_1) + \sum_{m=0}^{\infty}(2m+1)B_{nm}i_m(\kappa r_1)P_m(\cos\theta_1)] \qquad (A2)$$

where

$$B_{nm} = \sum_{\nu=0}^{\infty} A_{nm}^{\nu} k_{n+m-2\nu}(\kappa r) \tag{A3}$$

$$A_{nm}^{\nu} = \frac{\left(n+m-2\nu+\frac{1}{2}\right)}{\pi} \times \frac{\Gamma\left(n-\nu+\frac{1}{2}\right)\Gamma\left(m-\nu+\frac{1}{2}\right)\Gamma\left(\nu+\frac{1}{2}\right)}{\Gamma\left(n+m-\nu+\frac{3}{2}\right)} \times \frac{(n+m-\nu)!}{(n-\nu)!(m-\nu)!\nu!} \tag{A4}$$

In these expressions, r is the center-to-center distance between two particles, $\Gamma(x)$ is the gamma function, $P_n(x)$ is the Legendre polynomial of order n, and $i_n(x)$, and $k_n(x)$ are, respectively, the modified spherical Bessel functions of the first and the third kinds; $i_n(x)$ and $k_n(x)$ are related to the modified Bessel functions $I_{n+1/2}(x)$ and $K_{n+1/2}(x)$ by $i_n(x) = \sqrt{\pi/2x} I_{n+1/2}(x)$ and $k_n(x) = \sqrt{\pi/2x} K_{n+1/2}(x)$, respectively.

The coefficient α_n needs to be determined from the condition $\psi = \psi_1$ at $r_1 = R$. Substituting this condition into eq A2 and using the orthogonal property of Legendre polynomial, we obtain

$$([L] + [I])[A] = \psi_1[e] \tag{A5}$$

where

$$[L]_{jn} = (2j+1) B_{nj} \frac{i_j(\kappa R)}{k_n(\kappa R)} \tag{A6}$$

$$[A]_j = \alpha_j k_j(\kappa R) \tag{A7}$$

$$[I]_{ij} = \begin{cases} 1, j = i \\ 0, j \neq i \end{cases} \tag{A8}$$

$$[e]_j = \begin{cases} 1, j = 0 \\ 0, j > 0 \end{cases} \tag{A9}$$

Once α_0 is known, $u_{cc}(r)$ can be evaluated by eq 19.

Appendix B

In the liquid phase ($r_1 > R$ and $r_2 < R_s$), the solution to eq A1 can be expressed as[25]

$$\begin{aligned} \psi &= \sum_{n=0}^{\infty} [\alpha_n k_n(\kappa r_1) P_n(\cos\theta_1) + \beta_n i_n(\kappa r_2) P_n(\cos\theta_2)] \\ &= \sum_{n=0}^{\infty} [\alpha_n k_n(\kappa r_1) P_n(\cos\theta_1) + \beta_n \sum_{m=0}^{\infty} (2m+1) B_{nm,1} i_m(\kappa r_1) P_m(\cos\theta_1)] \\ &= \sum_{n=0}^{\infty} [\alpha_n \sum_{m=0}^{\infty} (2m+1) B_{nm,2} i_m(\kappa r_2) P_m(\cos\theta_2) + \beta_n i_n(\kappa r_2) P_n(\cos\theta_2)] \end{aligned} \tag{B1}$$

where

$$B_{nm,1} = \sum_{\nu=0}^{\infty} A_{nm}^{\nu} i_{n+m-2\nu}(\kappa r) \tag{B2}$$

$$B_{nm,2} = \sum_{\nu=0}^{\infty} A_{nm}^{\nu} k_{n+m-2\nu}(\kappa r) \tag{B3}$$

The definitions of the symbols are the same as those in Appendix A. Here, r denotes the distance between the center of a colloidal particle and that of the cavity. The unknown coefficients α_n and β_n in eq B1 need to be determined from the boundary conditions on the surfaces of particle and cavity.

If both the surface of a particle and that of cavity are remained at a constant potential, then applying the conditions $\psi = \psi_1$ at $r_1 = R$ and $\psi = \psi_2$ at $r_2 = R_s$, eqs B1−B3 lead to the following system of linear equations:

$$[I][a] + [L][b] = \psi_1[e] \tag{B4}$$

$$[M][a] + [I][b] = \psi_2[e] \tag{B5}$$

where the jth components of vectors $[a]$ and $[b]$ are

$$[a]_j = \alpha_j k_j(\kappa R) \tag{B6}$$

$$[b]_j = \beta_j k_j(\kappa R_s) \tag{B7}$$

The jnth elements of matrices $[L]$ and $[M]$ are

$$[L]_{jn} = (2j+1) B_{nj,1} i_j(\kappa R)/k_n(\kappa R_S) \tag{B8}$$

$$[M]_{jn} = (2j+1) B_{nj,2} i_j(\kappa R_s)/k_n(\kappa R) \tag{B9}$$

If the surface of a cavity is of charge-regulated nature and the electrical potential is sufficiently low, then we have the following general linear relation between the surface charge density σ and the surface potential ψ:

$$\sigma = S - K\psi \tag{B10}$$

where the sign of constant S is the same as that of the surface charge of the cavity when it is isolated. The constant K reflects the ability of a surface ionization reaction to maintain a constant surface charge, which is referred to as the regulation capacity of the surface.[22] If the relative permittivity of cavity is small, the surface charge density can be determined from the Gauss law as[27]

$$\sigma = -\epsilon \mathbf{n} \cdot \nabla\psi \tag{B11}$$

where $\mathbf{n}$ is the unit outward normal vector on cavity surface. Applying eqs B10 and B11 at $r_2 = R_s$ together with the condition $\psi = \psi_1$ at $r_1 = R$, we obtain the following system of linear equations for α_n and β_n:

$$[I][a] + [L][b] = \psi_1[e] \tag{B12}$$

$$[M][a] + [I][b] = \frac{R_s S}{\epsilon}[e] = \left(-1 - \kappa R_s + \frac{R_s K}{\epsilon}\right)\psi_2[e] \tag{B13}$$

where the jth components of vectors $[a]$ and $[b]$ are

$$[a]_j = \alpha_j k_j(\kappa R) \tag{B14}$$

$$[b]_j = \beta_j [(R_s K/\epsilon) k_j(\kappa R_s) + \kappa R_s k_j'(\kappa R_s)] \tag{B15}$$

The jnth elements of matrices $[L]$ and $[M]$ are

$$[L]_{jn} = (2j + 1)B_{nj,1}i_j(\kappa R)/[(R_sK_2/\epsilon)k_n(\kappa R_s) + \kappa R_s k_n'(\kappa R_s)] \quad \text{(B16)}$$

$$[M]_{jn} = (2j + 1)B_{nj,2}[(R_sK/\epsilon)i_j(\kappa R_s) + \kappa R_s i_j'(\kappa R_s)]/k_n(\kappa R) \quad \text{(B17)}$$

Note that these expressions involve ψ_2 and K only, that is, S is eliminated in their derivation.

Acknowledgment. This work is supported by the National Science Council of the Republic of China.

References and Notes

(1) Henderson, D. *Fundamentals of Inhomogeneous Fluids*; Marcel Dekker: New York, 1992.
(2) Cracknell, R. F.; Gubbins, K. E.; Maddox, M.; Nicholson, D. *Acc. Chem. Res.* **1995**, *28*, 281.
(3) Walz, J. Y.; Sharma, A. *J. Colloid Interface Sci.* **1994**, *168*, 485.
(4) Walz, J. Y. *J. Colloid Interface Sci.* **1996**, *178*, 505.
(5) Feigin, R. I.; Napper, D. H. *J. Colloid Interface Sci.* **1980**, *75*, 525.
(6) Chu, X. L.; Nikolov, A. D.; Wasan, D. T. *Langmuir* **1996**, *12*, 5004.
(7) Van Winkle, D. H.; Murray, C. A. *J. Chem. Phys.* **1988**, *89*, 3885.
(8) Hohenberg, P.; Kohn, W. *Phys. Rev. B* **1964**, *136*, 864.
(9) Hansen, J. P.; McDonald, I. R. *Theory of Simple Fluids*; Academic: New York, 1986.
(10) Choudhury, N.; Ghosh, S. K. *J. Chem. Phys.* **1999**, *111*, 1737.
(11) Chavez-Paez, M.; Acuna-Campa, H.; Yeomans-Reyna, L.; Valdez-Covarrubias, M.; Medina-Noyola, M. *Phys. Rev. E* **1997**, *55*, 4406.
(12) Hsu, J. P.; Tseng, M. T.; Tseng, S. *Chem. Phys.* **1999**, *242*, 69.
(13) Lozada-Cassou, M. *J. Phys. Chem.* **1983**, *87*, 3729.
(14) Zaini, P.; Modarress, H.; Mansoori, G. A. *J. Chem. Phys.* **1996**, *104*, 3832.
(15) Yeomans, L.; Feller, S. E.; Sanchez, E.; Lozada-Cassou, M. *J. Chem. Phys.* **1993**, *98*, 1436.
(16) Greathouse, J. A.; McQuarrie, D. A. *J. Phys. Chem.* **1996**, *100*, 1847.
(17) Patey, G. N. *J. Chem. Phys.* **1980**, *72*, 5763.
(18) Lozada-Cassou, M. *J. Chem. Phys.* **1984**, *80*, 3344.
(19) Lozada-Cassou, M.; Diaz-Herrera, E. *J. Chem. Phys.* **1990**, *93*, 1194.
(20) McQuarrie, D. A. *Statistical Mechanics*; Harper and Row: New York, 1976.
(21) Broyles, A. A.; Chung, S. U.; Sahlin, H. L. *J. Chem. Phys.* **1962**, *37*, 2462.
(22) Carnie, S. L.; Chan, D. Y. C.; Gunning, J. S. *Langmuir* **1994**, *10*, 2993.
(23) Sader, J. E.; Chan, D. Y. C. *J. Colloid Interface Sci.* **1999**, *213*, 268.
(24) Sader, J. E.; Chan, D. Y. C. *J. Colloid Interface Sci.* **1999**, *218*, 423.
(25) Langbein, D. *Theory of van der Waals Attraction*; Springer: Berlin, 1974.
(26) Marcelja, S.; Mitchell, D. J.; Ninham, B. W.; Sculey, M. J. *J. Chem. Soc., Faraday Trans. 2* **1977**, *73*, 630.
(27) Hunter, R. J. *Foundations of Colloid Science*; Oxford University Press: London, 1989; Vol. I.